Proceedings of IMECE2007
2007 ASME International Mechanical Engineering Congress and Exposition
November 11-15, 2007, Seattle, Washington, USA

IMECE2007-43494

NUMERICAL STUDY OF TIME DOMAIN APPROACH APPLIED TO PREDICTION OF NOISE RADIATION FROM ROTATING BLADES

G. TELLIER, D. FEDALA, S. KOUIDRI and R. REY
Laboratoire d'Energétique et de Mécanique des Fluides Interne,
Ecole Nationale Supérieure d'Arts et Métiers,
151, bd. de l'Hôpital, Paris, France, 75013
e-mail : djaafer.fedala@paris.ensam.fr

ABSTRACT

Aeroacoustic formulations in time domain are frequently used to model the aerodynamic sound of airfoils, the time data being more accessible. The formulation 1A developed by Farassat, integral solution of the Ffowcs Williams and Hawkings equation, holds great interest because of its adequacy for surfaces in arbitrary motion. The aim of this work is to study the numerical sensitivity of this model to specified parameters and the geometry used in the calculation. The numerical algorithms, spatial and time discretizations, and approximations used for far-field acoustic simulation are presented. A parametrical study of the relevant criteria is carried out based on the Isom's and Tam's test cases.

A helicopter blade airfoil as defined by Farassat to investigate the Isom's case is used in this work. According to Isom, the acoustic response of a dipole source with a constant aerodynamic load $\rho_0 c_0^2$ is equal to the thickness noise contribution. In practice, this observation is subject to numerical errors that are not systematically well controlled.
Variations of these errors depending on the time step, Mach number and the source-observer distance are studied. The analysis is then extended to the Tam's test case. Tam test case has the advantage of providing an analytical solution for the first harmonic.

NOMENCLATURE

c_0	ambient sound speed
dS	element of the control surface
$D(\theta)$	Tam's directivity in spherical coordinates
$f = 0$	function that describes the source surface
F_x, F_r, F_φ	Tam's forces in cylindrical coordinates
$H(f)$	Heaviside function
$J_m(\ )$	the m^{th}-order Bessel function
L_i	components of local force intensity that acts on the fluid, $L_i = \lfloor (p - p_0)\delta_{ij} - \tau_{ij} + \rho u_i (u_j - v_j) \rfloor n_j$
$\dot{L}_r$	$\frac{\partial L_i}{\partial \tau} \frac{r_i}{r}$
M	local Mach number vector of source with respect to a frame fixed to the undisturbed medium, with components M_i
$\dot{M}$	$\frac{\partial M_i}{\partial \tau}$
M_n	Mach number in direction normal to the surface, $M_i n_i$
M_r	Mach number of source in radiation direction, $M_i \hat{r}_i$
$\dot{M}_r$	$\dot{M}_i \hat{r}_i$
mtr	number of time steps per period
$\hat{n}$	unit outward normal vector to the surface, with components $\hat{n}_i$

Copyright © 2007 by ASME

$\tilde{p}$	far-field acoustic pressure
$\tilde{p}_L$	loading noise component
$\tilde{p}_T$	thickness noise component
P_{ij}	compressive stress tensor
r	source–observer distance, $r = \lvert x - y \rvert$
$\hat{r}$	unit vector in the radiation direction, with components $\hat{r}_i$
t	observer time
t_n	nth time step
T	blade passage time
T_{ij}	Lighthill stress tensor, $\rho u_i u_j + P_{ij} - c^2 \rho' \delta_{ij}$
u_i	components of local fluid velocity
v_n	local normal velocity of source surface
$v_{\dot{n}}$	$v_i \dot{\hat{n}}_i$
$\dot{v}_n$	$\dot{v}_i \hat{n}_i$
x	observer position vector, with components x_i
(x, r, φ)	cylindrical coordinates for Tam's test case
y	source position vector, with components y_i
$\delta(f)$	Dirac function
δ_{ij}	Kronecker delta
λ_{mN}	the N^{th} root of J'_m, that means $J'_m(\lambda_{mN}) = 0$
θ	the angle defined by the rotation axis and the source-observer direction
Ω	rotor angular velocity
ρ_0	density of the medium at rest
τ	source time (retarded time).

Indices:

$\dot{[]}$	the over dotted variables denote retarded temporal derivatives
$[]_r$	index denotes projection onto the source-observer direction
$[]_M$	index denotes projection on the Mach number vector.

INTRODUCTION

Noise reduction is one of the challenges that transportation industry has to face because of the clients demands as well as the increasing legal restrictions. The aim is to take into account noise constraints during the design process. For this, Direct Numerical Simulations allow an accurate noise prediction. However, such approach is still underdevelopment for simple geometries, flow around cavity and cylinder, and could not be used in an industrial design process or even applied to a realistic rotating machine because of their high computations resources requirements. An alternative technique consists of coupling accurate aerodynamic calculations, such as Large Eddy Simulation or Detached Eddy Simulation, and aeroacoustic analogy. The numerical simulation has to determine accurately the unsteady loading on the blades, which are to be fed into Ffowcs Williams and Hawkings integral formulations. Noise sources are only computed around the surface. Then, far field acoustic pressure can be calculated by the evaluation of integrals.

Significant theoretical and computational advancements have been achieved with developments of the time domain integral formulations. Today, almost all deterministic rotor noise predictions are based on time-domain integral formulations of the FW&H equation. The formulation 1A developed by Farassat [1], integral solution of the FW&H equation, holds great interest because of its adequacy for surfaces in arbitrary motion. Di Francescantonio [2] proposed a new boundary integral formulation, which does not require the non-penetration condition neither the calculation of the surface pressure normal derivative. Casalino [3] introduced the advanced time approach in the retarded time formulation 1A of Farassat. Then, algorithms gain in efficiency because no iterative solutions of the retarded time equation need to be performed. Ghorbaniasl and Hirsch [4] presented a series of validation test cases for Farassat's formulation.

The results are very sensitive to the algorithms, spatial and time discretizations, and approximations used for far-field acoustic simulation. A look forward in evaluation of the numerical errors resulting from implementation of formulation 1A is essential. In practical situations, computation codes have to be verified and validated by means of well-known test cases. The verification can be ideally carried by comparing the computations to analytical solutions; the numerical errors are calculated through the discrepancies between the numerical and analytical solutions.

In this paper, a parametrical study of the relevant criteria in numerical implementation of Farassat's formulation 1A is carried out based on two efficient test cases: the Isom's test [5] and the Tam's test BenchMark [6, 7]. According to Isom, the acoustic response of a moving dipole source with a constant aerodynamic load $\rho_0 c_0^2$ is equal to the thickness noise contribution. Hence, Isom gave a consistency test to validate aeroacoustic calculation codes. In practice, this observation is subject to numerical errors that are not systematically well controlled. Variations of these errors depending on the time step, Mach number and the source-observer distance are studied.

Tam test case has the advantage of providing an analytical solution for the first harmonic of the produced by a specific distribution of forces. The analysis is then completed with the Tam's test case. The numerical errors of integral extension from the near-field aerodynamic data to the acoustic far-field are mainly the so-called spatial and temporal discretization errors, which should be convergent to zero if the spatial and temporal resolutions are sufficiently refined. These two kinds of errors are confirmed in the present verification through the following procedures.

Copyright © 2007 by ASME

FORMULATION 1A : NUMERICAL IMPLEMENTATION

In this part, development of the J.E. Ffowcs Williams and D.L. Hawkings analogy [8] is carried out. The acoustic solver is based on the integral retarded time FW&H formulation 1A with permeable surfaces of Di Francescantonio [9] and Brentner & Farassat [10, 11]. The interest of this formulation lies in the fact that time derivative of the integral terms of FW&H has been eliminated. Moreover, the evaluation of the noise can be done even if the observer is moving. The thickness and the loading noise of a surface in arbitrary motion is given as:

$$\begin{cases} \tilde{p}_T(\vec{x},t) = \tilde{p}_{T1}(\vec{x},t) + \tilde{p}_{T2}(\vec{x},t) \\ \\ \tilde{p}_L(\vec{x},t) = \tilde{p}_{L1}(\vec{x},t) + \tilde{p}_{L2}(\vec{x},t) + \tilde{p}_{L3}(\vec{x},t) \end{cases} \quad (1)$$

so,

$$\tilde{p}(\vec{x},t) = \tilde{p}_T(\vec{x},t) + \tilde{p}_L(\vec{x},t) \quad (2)$$

Where:

$$4\pi\,\tilde{p}_{T1}(\vec{x},t) = \oint_{f(\vec{y},\tau)=0}\left[\frac{\rho_0\left(\dot{U}_n + U_{\dot{n}}\right)}{rD^2}\right]_{\tau=t-r/c_0} dS \quad (3)$$

$$4\pi\,\tilde{p}_{T2}(\vec{x},t) = \oint_{f(\vec{y},\tau)=0}\left[\frac{\rho_0 U_n\left(r_i\dot{M}_i + c_0(M_r - M^2)\right)}{r^2D^3}\right]_{\tau=t-r/c_0} dS \quad (4)$$

and:

$$4\pi\,\tilde{p}_{L1}(\vec{x},t) = \frac{1}{c_0}\oint_{f(\vec{y},\tau)=0}\left[\frac{\dot{L}_r}{rD^2}\right]_{\tau=t-r/c_0} dS \quad (5)$$

$$4\pi\,\tilde{p}_{L2}(\vec{x},t) = \oint_{f(\vec{y},\tau)=0}\left[\frac{L_r - L_M}{r^2D^2}\right]_{\tau=t-r/c_0} dS \quad (6)$$

$$4\pi\,\tilde{p}_{L3}(\vec{x},t) = \frac{1}{c_0}\oint_{f(\vec{y},\tau)=0}\left[\frac{L_r\left(r\dot{M}_r + c_0(M_r - M^2)\right)}{r^2D^3}\right]_{\tau=t-r/c_0} dS \quad (7)$$

$\tilde{p}$ is the acoustic pressure, $\vec{x}$ being the observer position and $\vec{y}$ the source position so $r = |\vec{x} - \vec{y}|$ is the source-observer distance, $D = 1 - M_r$ the Doppler factor, L the aerodynamic pressure force $L_i = \left[(p - p_0)\delta_{ij} - \tau_{ij} + \rho u_i(u_j - v_j)\right]n_j$, τ_{ij} : the viscosity stress tensor and δ_{ij} : Kronecker symbol. ρ_0 and c_0 are respectively the density of the fluid and the sound speed in a medium at rest. v_i is the velocity of the surface control and u_i represents the fluid velocity so $U_i = \frac{\rho u_i}{\rho_0} + \left(1 - \frac{\rho}{\rho_0}\right)v_i$.

When the control surface is solid, the relative velocity $(u_j - v_j) = 0$.

It is important to point out that the terms between the brackets of equations (3-7) are evaluated at delayed time. The retarded-time integrals are approximated by mid-panel-quadrature algorithm. Values of physical variables Q are approximated at panel centroids y_j as :

$$4\pi\,\phi(\vec{x},t) \approx \sum_{i=1}^{N}\left(\sum_{j=1}^{n_i}\left[\frac{Q\left(y_j, t - r_j/c_0\right)}{r_j\left|1 - M_r\right|_j}\right]_{ret}\right)\Delta S_i \quad (8)$$

their evaluations are carried out with the source time regarded as the primary time (i.e., dominant). The source time for a panel is chosen and determines when the signal will reach the observer. The second then the fourth order Runge-Kutta equidistant derivation are used in this work for the calculation of $\dot{L}_i$ based on the inputs of $p(t)$.

If the observer is static, τ being the emission time, then the expression of time reception is basically :

$$t = \tau + \frac{r(\tau)}{c} \quad (9)$$

The signal is the summation of all computed values of disturbances emitted by the sources at different retarded times and reaching the observer at a unique observer time. Thus, an interpolation of the acoustic pressure at reception time is performed with spline algorithm so that the contributions from all source panels can be summed at the same observer times.

For a moving observer an expression of the advanced time has been given by Casalino [3].

ISOM TEST-CASE

Firstly, the Isom [5] test is reviewed. It has been shown that if a constant aerodynamic load $\rho_0 c_0^2$ is applied over a moving surface, then generated thickness noise and loading noise could be equal. This assumption can be demonstrated applying the wave operator at the generalized function $\rho_0 c_0^2\left[1 - H(f)\right]$ that is always equal to zero out of the surface defined by $f = 0$. Then,

$$\frac{\partial}{\partial t}[\rho_0 \upsilon_n \delta(f)] = -\frac{\partial}{\partial x_i}[\rho_0 c_0^2 n_i \delta(f)], \quad (10)$$

the mathematical form of thickness noise, left side, and loading noise, right side, are recognized. A more complete

Copyright © 2007 by ASME

demonstration can be found in [5, 12]. This analytical result is not always exact when applied numerically due to the differences of robustness in the integration of the two noises. This difference is affected by several geometrical and physical parameters of which the influence is not well studied.

A conventional rotor has been defined for the Isom's test case. The same helicopter rotor as defined by Farassat to study the Isom's case is used in this work. It is composed of 2 blades, Figure 1, of 4 m spanwise length for an external diameter of 10 m. The blades are symmetrical biconvex airfoil with a 10% thickness ratio (a NACA0010 profile is used in this work). The main chord is equal to 0.4 m.

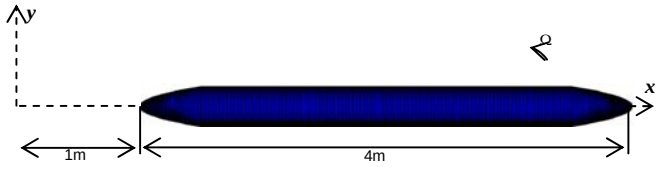

a)

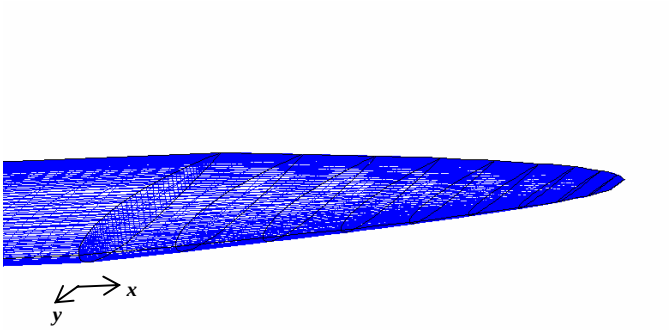

b)

Fig. 1: a) Used blade geometry b) Zoom on the tip, the thickness ratio is decreasing at the extremities of the blade.

In their first calculations, Farassat et al. [13] did not take into account the tips and the inner faces and the results did not agree with the theory. Then, they found that blade tip is an effective noise generation area when Isom's thickness noise formulae was studied [14]. This being corrected, a non negligible discrepancy remained especially at low tip Mach numbers. Their first idea was to refine the grid at the inner and outer radii of the blade. Thus, the quality of the results is improved. Last amelioration consists in decreasing the thickness ratio at the extremities of the blade, as shown in Figure 1. Once these ameliorations done, the result is excellent. Here appears the need of studying effect of these criteria. They will depend on the accuracy of the program computing the formulation F1A and are not unique. They will traduce the robustness of the program. Firstly, the results obtained for 0.4 and 0.8 tip Mach number with the code developed during this study for the blade shown in figure 1. are presented in figure 2. The observer is located in the rotation plane at 50 m away from the rotation axis. A good agreement is noticed between the Isom and monopole noise.

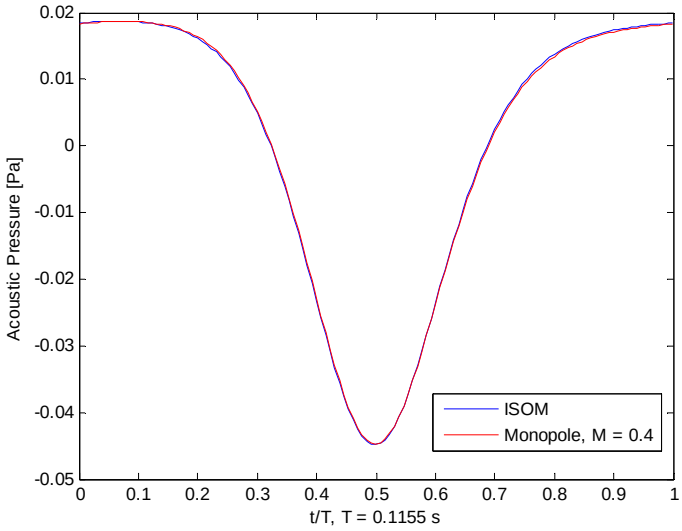

a)

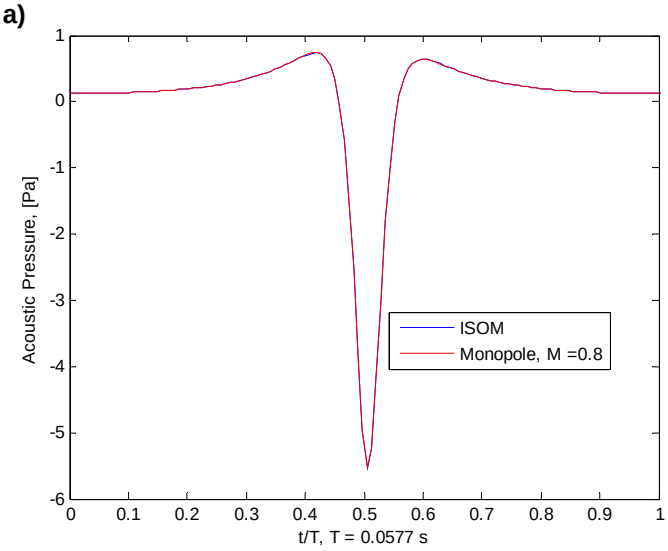

b)

Fig. 2 : Acoustic pressure signatures for a two-bladed rotor, **a)** Tip Mach number 0.4 **b)** Tip Mach number 0.8 .

DEFINITION OF THE ERROR

In order to compare the results obtained when parameters are varied, an accurate definition of the error is required. This definition must allow for studying the Mach number, the time step, and the source-observer distance effects. For Isom's test case, two sets of values must be compared $\tilde{p}_L$ and $\tilde{p}_T$ whereas, for Tam's benchmark, the comparison is carried out between analytical and numerical solutions. The relative error E_r takes into account the differences of scales

Copyright © 2007 by ASME

(magnitude), its definition for the comparison of loading and thickness noises at each time step is:

$$E_r(t_n) = \frac{\left|\tilde{p}_T(t_n) - \tilde{p}_L(t_n)\right|}{\max\left(\left|\tilde{p}_T(t_n)\right|;\left|\tilde{p}_L(t_n)\right|\right)} \quad (11)$$

In order to evaluate the discrepancy between two curves, the error considered is the arithmetical mean of the time relative errors:

$$\overline{E}_r = \frac{1}{mtr} \cdot \sum_{t=t0}^{T} E_r(t_n) \quad (12)$$

An absolute error could also be used :

$$E_a = \frac{1}{mtr} \cdot \sum_{t=t0}^{T} \left|\tilde{p}_T(t_n) - \tilde{p}_L(t_n)\right| \quad (13)$$

TIME STEP AND ORDER OF THE DERIVATION

The first parameter studied is the number of time steps per one rotation period. Figure 3. presents the mean relative error depending on the number of time steps used in the computation. The previous geometry is kept with the same mesh grid, the observer is in the rotation plane, and only the number of time steps per one rotation period is varied. Two differentiation algorithms used in the computation of $\dot{L}$ are compared: second order (RK 2) and fourth order Runge Kutta equidistant derivation scheme (RK 4), the tip Mach number is fixed here to 0.8.

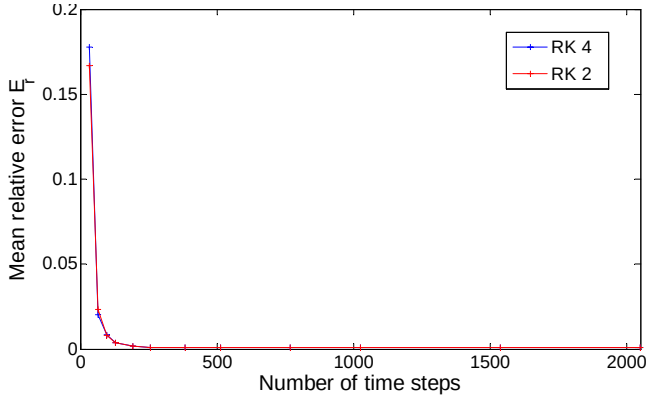

Fig. 3: Time step and order of the derivation.

The error is decreasing when the number of time steps per one rotation period is increasing. For the presented configuration, 512 time steps are sufficient to give a minimal error. This value is used for all the following computations. Although the order of the scheme used is not relevant in this case, the fourth order Runge Kutta equidistant derivation scheme is kept for the rest of computations. For practical configurations, carrying out this test should give the minima of the number of time steps needed to have a possible accurate acoustic solution.

SOURCE-OBSERVER DISTANCE

The parameter considered here is the source-observer distance. Even if theoretically the formulation F1A is adequate to predict aeroacoustic noise in near-field domain, as noticed in Farassat [10], the numerical results are sensitive to source-observer distance.

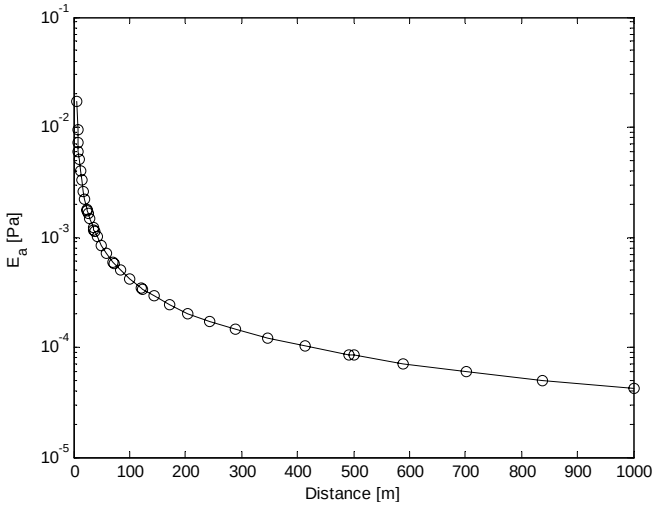

Fig. 4: Absolute error function of the source-observer distance.

In figure 4, the absolute error depending on the source observer distance is presented. The discrepancies decrease when the observer is in the far field. When the mean relative error $\overline{E}_r$ is considered, figure 5, although a minimum is noticed around 250 m, the discrepancy between loading noise and thickness noise is nearly not varying in relative value staying between 0.54 and 0.57%.

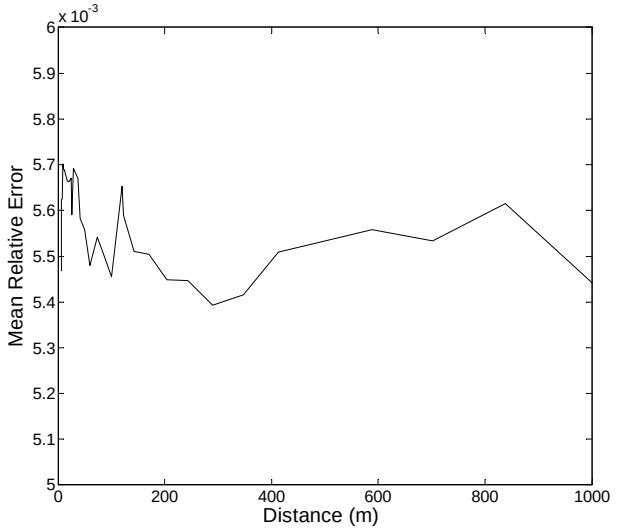

Fig. 5: Relative error $\overline{E}_r$ over the source observer distance.

Copyright © 2007 by ASME

In other terms, the integrals in 1/r (far field domain) and 1/r² (near field domain) are estimated with the same accuracy. Source-observer distance is not a source of error and presented numerical scheme describes far field domain noise generation as well as near field confirming the adequacy to predict the aeroacoustic noise in near-field domain.

DIRECTIVITY

In order to study the directivity, the observer is located at 50 m away from the rotation centre and the angle defined by observer position vector and the rotation plane is varied, 0° angle corresponds to observer position at the rotation plane. The tip Mach number is fixed to 0.8. The number of time steps per rotation period is 512. Figure 6. a) shows the maximum of $\tilde{p}_T$ and $\tilde{p}_L$ over one period depending on the rotation angle. The directivity feature shows a dipolar character.

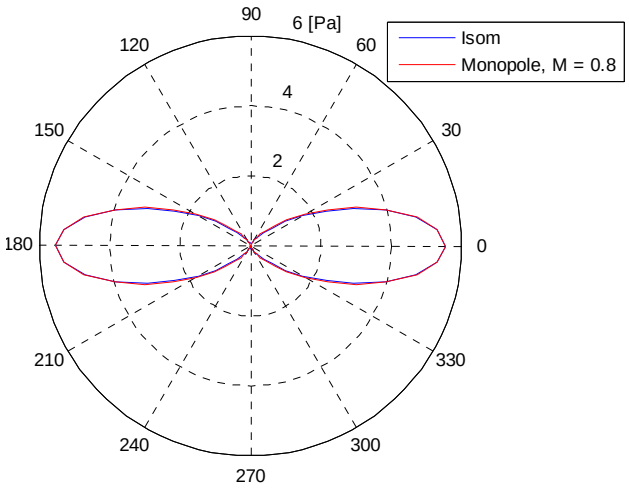

a)

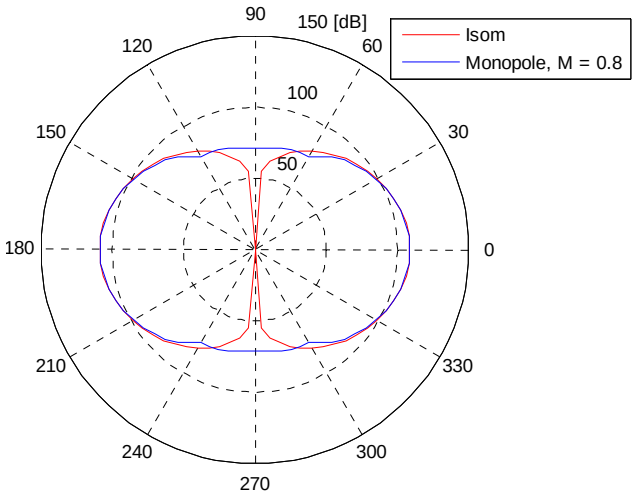

b)

Fig. 6: Directivity of the maximum of isom and thickness noise $\tilde{p}_T$ and $\tilde{p}_L$ over one period **a)** [Pa] **b)** dB, p_{ref}=2 10^{-5} Pa

Acoustic pressures found are maxima in the rotation plane. On other hand, the acoustic pressure is minima along the rotation axis. In the rotation axis, the tangential aerodynamics forces are not responsible on noise emission in the axis. Only the axial forces can generate noise in the rotation axis.

The look at the relative error depending on the angle θ_{dir}, figure 7, brings out that the regions with maximum relative error are those with the minimum acoustic pressures. For some values of θ_{dir}, $\overline{Er}$ is nearly equal to 1, that means near the rotation axis, the error is significant. One could think that the large error shown in figure 7 at rotation axis has no real significance in that the acoustic pressures at these locations are nearly zero, figure 6 a). However, the look at acoustic pressure levels, figure 6 b), illustrate that these errors are physically consistent; the range of the pressure levels are important.

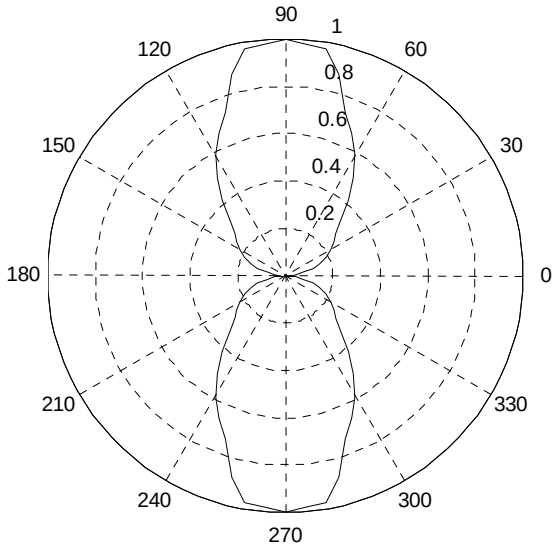

Fig. 7: Directivity of the mean relative error $\overline{E}_r$.

MACH NUMBER

As noticed by Farassat [10], for subsonic motions, the discrepancy between Isom's noise and thickness noise increases when Mach number is decreasing. A good illustration is given on figure 8 for 0.2 tip Mach number. The used parameters are the same as those in computing of the results for 0.4 and 0.8 Mach numbers (figure 2).

Copyright © 2007 by ASME

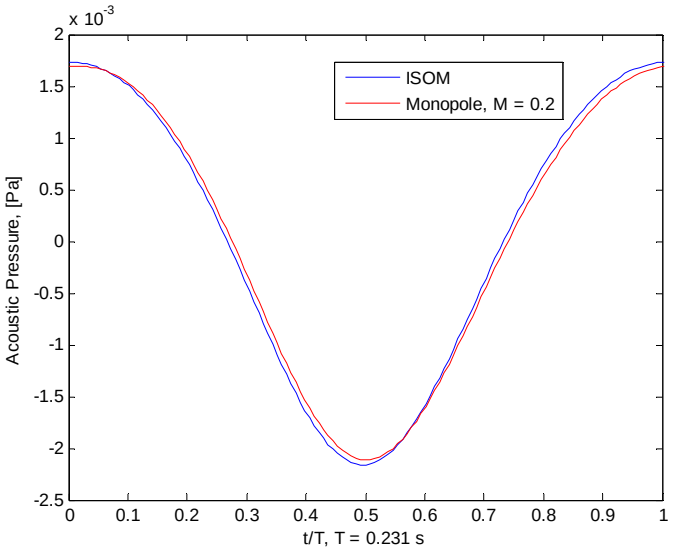

Fig. 8: Acoustic pressure signatures for a two-bladed rotor, tip Mach number 0.2 .

The evolution of the relative error depending on the Mach number is represented in figure 9,. The mean relative error decreases when the Mach number is increasing. This result suggests that the mesh grid has to be refined near the regions moving at low Mach number, i-e near the inner radius.

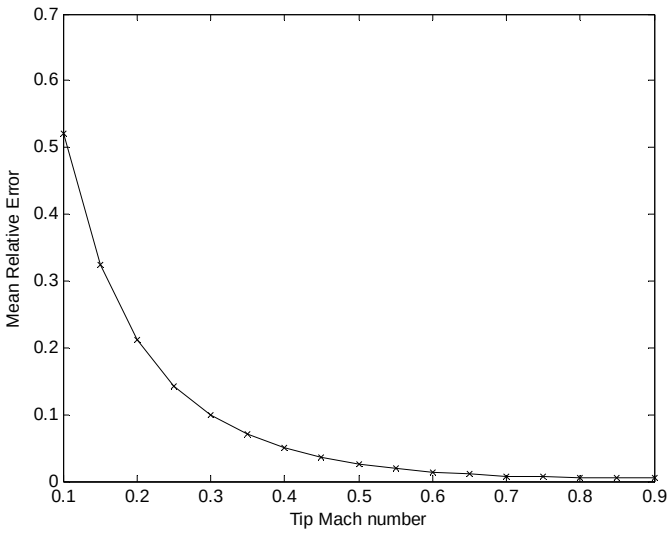

Fig. 9: Mean relative error $\overline{E}_r$ over tip Mach number.

TAM TEST CASE

The second test case studied in this work has been provided by Tam [6]. It is the exact solution of the linearized Euler equations for the first harmonic of the noise produced by a specific distribution of forces. This test has been described in the third CAA benchmark problems workshop [7]. The geometrical configuration is shown in figure 10: the rotor is 1.6m long and its radius is 1m.

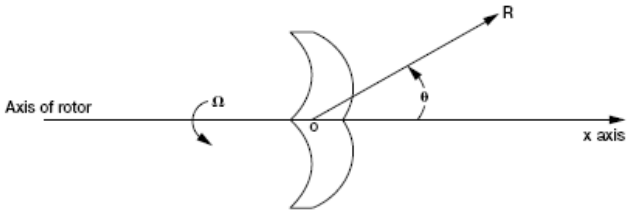

Fig. 10: Tam's open rotor.

In this section the variables are non-dimensionalized with respect to the following scales :

length scale : b , length of the blade
velocity scale : c_0 , ambient sound speed
time scale : $\frac{b}{c_0}$
density scale : ρ_0 , ambient fluid density
pressure scale : $\rho_0 c_0^2$
body force scale : $\frac{\rho_0 c_0^2}{b}$

The physical rotor is replaced in a cylindrical coordinates (x, r, φ) by the following distribution of forces:

$$\begin{bmatrix} F_r(r,\varphi,x,t) \\ F_\varphi(r,\varphi,x,t) \\ F_x(r,\varphi,x,t) \end{bmatrix} = \mathrm{Re}\left\{ \begin{matrix} 0 \\ \tilde{F}_\varphi(r,x) \\ \tilde{F}_x(r,x) \end{matrix} \right\} e^{im(\varphi-\Omega t)} \quad (14)$$

where

$$\tilde{F}_\varphi(r,x) = \begin{cases} F(x)\, r\, J_m(\lambda_{mN} r) & r \le 1 \\ 0 & r > 1 \end{cases}$$

$$\tilde{F}_x(r,x) = \begin{cases} F(x)\, J_m(\lambda_{mN} r) & r \le 1 \\ 0 & r > 1 \end{cases}$$

$$F(x) = \exp\left\{ -(\ln 2)(10x)^2 \right\}$$

and $J_m(\ )$ is the m^{th}-order Bessel function, λ_{mN} is the N^{th} root of J'_m, that means $J'_m(\lambda_{mN}) = 0$. The calculation has been made for an 8 blade rotor, so m = 8 and setting N = 1 (λ_{mN} = 9.64742). Ω, as every variable is nondimensional.
Tam showed that the acoustic pressure, the frequency of the radiated sound is the first harmonic $m\,\Omega$, can be approached by

$$\tilde{p}(R,\theta,t) \underset{R\to\infty}{\approx} \frac{2}{R} A(k_S) e^{im\Omega(R-t) - \frac{i}{2}(m+1)\pi} \quad (15)$$

Copyright © 2007 by ASME

where

$$A(k_S)=\frac{1}{4}\left(\frac{\pi}{100\ln 2}\right)^{\frac{1}{2}}\frac{m^2(1+\Omega\cos\theta)\Omega\sin\theta}{\lambda_{mN}^2-m^2\Omega^2\sin^2\theta}J_m(\lambda_{mN})J'_m(m\Omega\sin\theta)e^{-\frac{m^2\Omega^2\cos^2\theta}{400\ln 2}} \quad (16)$$

and $k_s = m\Omega\cos\theta$.

It is to highlight that in equation (13) from reference [5], giving $A(k_S)$, there is an error certainly typographical: instead of $m\Omega\sin\theta$ it is written as $mR\sin\theta$. The directivity $D(\theta)$ in spherical coordinates is defined as :

$$\mathrm{D}(\theta)=\lim_{R\to\infty}R^2\overline{\tilde{p}^2(R,\theta,\varphi,t)}=2A^2(k_S) \quad (17)$$

The over-bar denotes the time average. In order to test the code based on the FWH equation, Tam's benchmark problem was adapted by Hirsch et al [4, 15] by removing the harmonic exponential dependence of the blade force. A new blade force was defined as :

$$\begin{bmatrix}F_r(r,\varphi,x,t)\\F_\varphi(r,\varphi,x,t)\\F_x(r,\varphi,x,t)\end{bmatrix}=\mathrm{Re}\left\{\begin{matrix}0\\\tilde{F}_\varphi(r,x)\\\tilde{F}_x(r,x)\end{matrix}\right\} \quad (18)$$

The aerodynamic forces defined in equation (18) are substituted in the loading noise sources of formulation 1A. The first harmonic of the computed solution should be identical to Tam's analytical solution. Firstly, the results given by Tam [6] are reproduced by the acoustic solver developed in this work. As the problem is axisymmetric about the x axis the computational domain is defined in the r-x plane as $-0.8 \le x \le 0.8$ and $0 \le r \le 1$. The blade surface is discretized into equally spaced points (40 points along x axis × 25 points along r axis). Figure 11. shows the results obtained for Ω = 0.85 at R = 100 m. On figure 11. a) is represented the computed dipole far-field acoustic pressure with F1A at (θ = 90° and R = 100 m, Ω = 0.85).

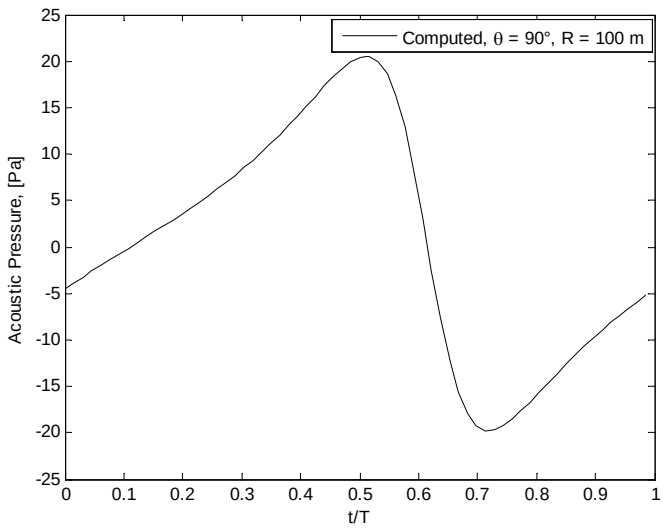

a)

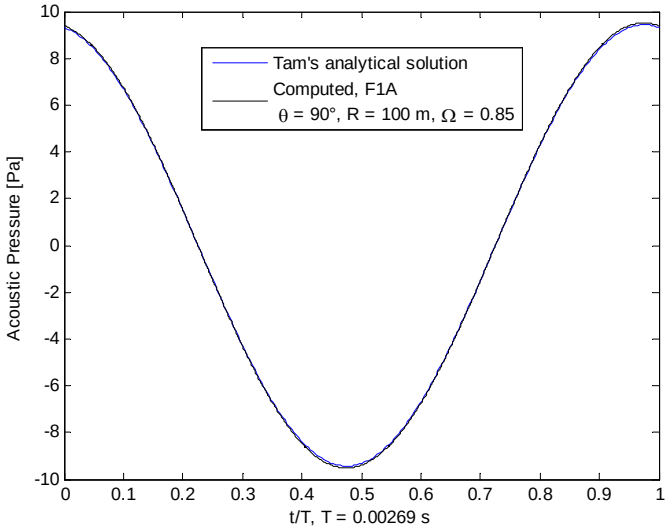

b)

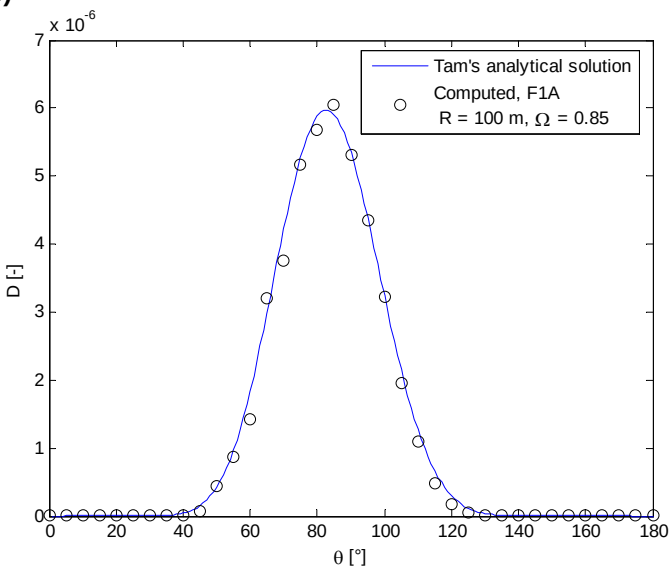

c)

Fig. 11: Results for Ω = 0.85: **a)** Computed dipole acoustic pressure with F1A, **b)** Computed first harmonic signal with F1A compared to Tam's analytical solution, equation (15). **c)** Computed first harmonic directivity with F1A compared to Tam's analytical solution, equation (17).

The first harmonic of this signal is compared to Tam's analytical solution on figure 11 b). The computed directivity of the first harmonic is presented on figure 11 c). The results are agreeing perfectly. This suggests that the numerical method predicts the dipole noise accurately at Ω = 0.85.

The same results are presented in figure 12. for $\Omega = 0.6$. Some discrepancies are noticed and the concordance is less significant. These results reinforce those obtained in studying the Mach number effect for Isom's test case.

Copyright © 2007 by ASME

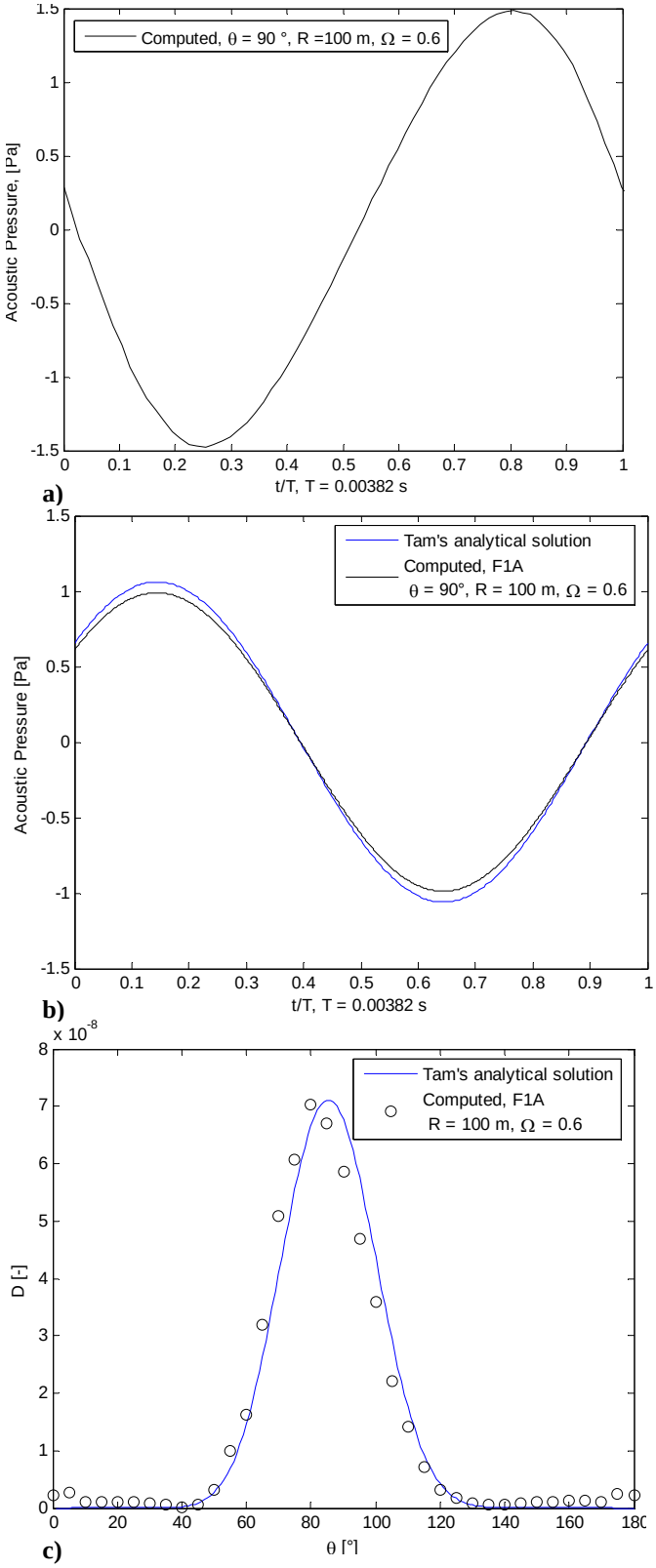

Fig. 12: Results for $\Omega = 0.6$: **a)** Computed dipole acoustic pressure with F1A, **b)** Computed first harmonic signal with F1A compared to Tam's analytical solution. **c)** Computed first harmonic directivity with F1A compared to Tam's analytical solution

CONCLUSION :

Development of the J.E. Ffowcs Williams and D.L. Hawkings analogy is carried out. The acoustic solver is based on the integral retarded time of Formulation 1A developed by Brentner and Farassat. The retarded-time integrals are approximated by mid-panel-quadrature algorithm. They are calculated with the source time regarded as the primary time (i.e., dominant). The second then the fourth order Runge-Kutta equidistant derivation are used for the evaluation of aerodynamic loadings. An interpolation of the acoustic pressure at the reception time is performed with spline algorithm so that the contributions from all source panels are summed at the same observer times.

A parametrical study of the relevant criteria is carried out based on the Isom's and Tam's test cases. In order to compare the results obtained when parameters are varied, a relative average error definition is introduced. This definition allowed for studying the effects of Mach number, the time step, and the source-observer distance. For Isom's test case, thickness noise is compared to loading noise whereas, for Tam's benchmark, the comparison is performed between analytical and numerical solutions.

The same helicopter rotor as defined by Farassat to study the Isom's case is used. The obtained results show that the error is decreasing when the number of time steps per one rotation period is increasing. For the presented configuration, 512 time steps are sufficient to give a minimal error for 0.8 tip Mach number. For practical configurations, carrying out this test should give the minima of the number of time steps needed to have a possible accurate acoustic solution.

Even if theoretically the formulation F1A is adequate to predict the near-field aerodynamic noise, the numerical results are sensitive to source-observer distance. The absolute error decrease when the observer is in the far field. However, the discrepancy between loading noise and thickness noise is nearly not varying in relative values. In other terms, the integrals in $1/r$ (far field domain) and $1/r^2$ (near field domain) are estimated with the same accuracy.

The directivity feature shows a dipolar character. Acoustic pressures found are maximum in the rotation plane. On other hand, the acoustic pressure is minima along the rotation axis. In the rotation axis, the tangential aerodynamics forces are not responsible on noise emission in the axis. Only the axial forces can generate noise in the rotation axis.

The mean relative error decreases when the Mach number is increasing. This result suggests that the meshgrid has to be refined near the regions moving at low Mach number.

The analysis is then extended to the Tam's test case. The results are agreeing perfectly in case of $\Omega = 0.85$. Whereas, for $\Omega = 0.6$, some discrepancies are noticed confirming that the errors increase when tip Mach number is decreasing.

Copyright © 2007 by ASME

ACKNOWLEDGEMENT

The authors would like to thank Pr. Hirsch for suggesting the Isom thickness case as a verification base.

REFERENCES

[1] Brentner, K. S., Farassat, F., 1998, “Analytical Comparison of the Acoustic Analogy and Kirchhoff Formulation for Moving Surfaces”, AIAA J., 36(8), 1379-1386

[2] Di Francescantonio, P., 1997, “A New Boundary Integral Formulation for the Prediction of Sound Radiation”, Journal of Sound and Vibrations, 202(4), pp. 491–509.

[3] Casalino, D., 2003, , “An Advanced Time Approach for Aeroacoustic Analogy Predictions”, Journal of Sound and Vibrations, 261, pp. 583–612.

[4] Ghorbaniasl, G., Hirsch, C., 2005, “Validation and Application of a Far-Field Time Domain Formulation for Fan Noise Prediction”, 11th AIAA/CEAS Aeroacoustics Conference, AIAA 2005-2838.

[5] Isom, M. P., 1975, “The Theory of Sound Radiated by a Hovering Transonic Helicopter Blade”, Poly-AE/AM, No. 75-4, Polytechnic Institute of New York.

[6] Tam, C., 2000, ”Rotor noise: Category 2, Benchmark problems”, Third Computational Aeroacoustics (CAA) Workshop on Benchmark Problems, NASA/CP-2000-209790.

[7] Tam, C., 2000, ”Rotor noise: Category 2, Analytical solution”, Third Computational Aeroacoustics (CAA) Workshop on Benchmark Problems, NASA/CP-2000-209790.

[8] Ffowcs Williams, J. E. and Hawkings, D. L., 1969, **“**Sound Generated by Turbulence and Surfaces in Arbitrary Motion”, Philosophical Transactions of the Royal Society, A264, 321-342.

[9] Di Francescantonio, P., 1997, “A New Boundary Integral Formulation for the Prediction of Sound Radiation”, J. Sound Vib. 202(4), pp 491-509.

[10] Brentner, K. S., Farassat, F., 1998, **“**Analytical Comparison of the Acoustic Analogy and Kirchhoff Formulation for Moving Surfacessurfaces”, AIAA J., 36(8), 1379-1386.

[11] Brentner, K. S., Farassat, F., 2003, **“**Modeling Aerodynamically Generated Sound of Helicopter Rotors”, Progress in Aerospace Sciences, Vol. 39, 83-120.

[12] Farassat, F., 1979, “The Derivation of a Thickness Noise Formula for The Far-Field by Isom”, Journal of Sound and Vibrations, 64(1), pp. 159–160.

[13] Farassat, F., 1980, “Isom’s Thickness Noise Formula for Rotating Blades with Finite Thickness at The Tip”, Journal of Sound and Vibrations, 72(4), pp. 550–553.

[14] Farassat, F., Martin, R., 1982, “A Note on the Tip Noise of Rotating Blades”, Journal of Sound and Vibrations, 86(3), pp. 449–453.

[15] Hirsch, Ch., Ghorbaniasl, Gh., and Ramboer, J., “Fan Noise Simulation in the Time Domain: Validation Test Cases”, The Second International Symposium on Fan Noise (Senlis (France)), 2003

 Copyright © 2007 by ASME